J Mater Sci (2007) 42:8811–8823
DOI 10.1007/s10853-007-1917-y

A continuum model for remodeling in living structures

Ellen Kuhl · Gerhard A. Holzapfel

Received: 29 December 2006 / Accepted: 4 June 2007 / Published online: 14 July 2007

Abstract A new remodeling theory accounting for mechanically driven collagen fiber reorientation in cardiovascular tissues is proposed. The constitutive equations for the living tissues are motivated by phenomenologically based microstructural considerations on the collagen fiber level. Homogenization from this molecular microscale to the macroscale of the cardiovascular tissue is performed via the concept of chain network models. In contrast to purely invariant-based macroscopic approaches, the present approach is thus governed by a limited set of physically motivated material parameters. Its particular feature is the underlying orthotropic unit cell which inherently incorporates transverse isotropy and standard isotropy as special cases. To account for mechanically induced remodeling, the unit cell dimensions are postulated to change gradually in response to mechanical loading. From an algorithmic point of view, rather than updating vector-valued microstructural directions, as in previously suggested models, we update the scalar-valued dimensions of this orthotropic unit cell with respect to the positive eigenvalues of a tensorial driving force. This update is straightforward, experiences no singularities and leads to a stable and robust remodeling algorithm. Embedded in a finite element framework, the algorithm is applied to simulate the uniaxial loading of a cylindrical tendon and the complex multiaxial loading situation in a model artery. After investigating different material and spatial stress and strain measures as potential driving forces, we conclude that the Cauchy stress, i.e., the true stress acting on the deformed configuration, seems to be a reasonable candidate to drive the remodeling process.

E. Kuhl (✉)
Department of Mechanical Engineering, Stanford University, Stanford, CA 94305, USA
e-mail: ekuhl@stanford.edu

G. A. Holzapfel
Department of Solid Mechanics, School of Engineering Sciences, Royal Institute of Technology, Stockholm 100 44, Sweden

G. A. Holzapfel
Institute for Biomechanics, Center for Biomedical Engineering, Graz University of Technology, Graz 8010, Austria

Introduction and motivation

Living tissues are able to adapt to physiological and pathophysiological stimuli in order to keep adequate perfusion according to the metabolic demand of the tissue. For example, changes in mechanical stimuli lead to altered cellular and extracellular activities, and typical observed biological responses are related to growth, remodeling, adaptation, and repair, i.e., mechanobiology (see, e.g., Humphrey [33], Huang et al. [31], Ingber [34], Klein-Nulend et al. [35], Wang and Thampatty [55], Holzapfel and Ogden [28, 29], Mofrad and Kamm [47] or Lehoux et al. [40]). Changes in the material (and structural) properties of, for example, the artery wall through alterations in its internal microstructure constitute an active process that occurs in response to changes of mechanical parameters, a process called 'arterial remodeling.' It is the endothelium cell that sense mechanical and humoral parameters, transduce signals to the underlying smooth muscle cells and to the surrounding tissue, and relay mechanical and biochemical changes into biomolecular events. Therefore, the endothelium at the interface of the blood plays a crucial role in the initiation of arterial remodeling. In particular, in cardiovascular tissues, remodeling processes are important

in the context of arterial development, atherosclerosis, and healing in response to arterial injury. A great deal of interdisciplinary research effort is devoted to the (mechanical) signaling pathways because they may enable the identification of therapeutic targets and the development of new pharmacological strategies. Moreover, understanding the interplay between the architecture of the internal microstructure and the mechanical loading is of fundamental importance to engineer, e.g., blood vessel substitutes, see Nerem and Seliktar [48].

The function and integrity of organs are maintained by the tension in collagen fibers, which contribute significantly to the stability and strength of organs. Collagen fibers are typically considered as the main load bearing constituent of the extracellular matrix. Accordingly, changes in the material (and structural) properties can primarily be attributed to variations in collagen content, type and thickness and, of course, in the orientation within the tissue. Leung et al. [41, 42] were amongst the first to verify experimentally that mechanical forces relate to pressure and flow direct medial cell biosynthesis and modulate structural adaptations to hemodynamic changes. Based on in vitro studies of smooth muscle cells, they reported that aortic medial cells attached to elastic membranes and subjected to cyclic stretching consistently synthesized collagen of types I and III much more rapidly than did cells growing on stationary membranes. In the present manuscript we use the word 'remodeling' exclusively with respect to collagen fiber reorientation, while the type and thickness of collagen as well as its content and its concentration are assumed to be constant. In addition, we do not address adaptation in the form of volumetric growth which is addressed in detail elsewhere in the literature, see, e.g., Rodriguez et al. [49], Lubarda and Hoger [43] or Kuhl et al. [38]. There is, however, strong evidence that growth and remodeling can indeed be viewed as separate individual processes. Stopak and Harris [50] studied the orientation of collagen fibrils due to the forces exerted on them by fibroblast in gels. Fiber reorientation was found to take place in response to changes in the mechanical loading although no significant growth, resorption, and production of new fibers was reported. Motivated by these findings, Garikipati et al. [20] provided a theoretical framework that focuses exclusively on collagen fiber remodeling and supported their theory by a set of remodeling experiments. For a more sophisticated theoretical approach that captures the interaction of the individual phenomena of growth and remodeling, the reader is referred to Menzel [45].

To gain further insight into the complex biomechanical phenomena related to tissue remodeling we aim at formulating and implementing a novel constitutive framework for collagen fiber remodeling with particular emphasis on the arterial wall, in which type I collagen is the major constituent. As such, the central focus of this study is to capture, predict and explain basic trends observed in collagen fiber remodeling and its impact on the structural response at the tissue or organ level. There seems to be a general agreement that the interplay between matrix stress, fibroblast alignment and stress in the actin network is responsible for collagen fibril reorientation as reported by Stopak and Harris [50] and described in detail by Garikipati et al. [20]. However, we do not aim at explaining the origin of remodeling which is governed by many highly complex interactive phenomena on the cellular level that involve altered gene expression in response to altered loading (i.e., gene transcription, translation, protein synthesis, packing, and activation) which eventually results in altered rates of turnover of cells and matrix. Nor do we aim at following the classical continuum mechanics approach and develop a purely invariant based macroscopic theory governed by a number of abstract material parameters. Our goal is to apply suitable homogenization techniques to derive a sound phenomenologically and micromechanically based formulation with a limited number of parameters that have a clear physical interpretation.

To this end, we begin our investigations on the microstructural or rather molecular level focusing on the mechanical description of the individual collagen fibers. The characteristic feature of typical collagen molecules is their long, stiff, triple-stranded helical structure in which three collagen polypeptide chains are wound around one another in rope-like superhelical structures which are stabilized by numerous hydrogen bonds. The mechanical properties of these helical structures are unlike those of any other natural or synthetic polymers. Collagen helices display a remarkable stiffness which may be characterized appropriately through the so-called wormlike chain model. The wormlike chain, or rather Kratky and Porod model [36], imagines the polymer as a rod that bends smoothly under thermal fluctuations. Traditionally applied to model the DNA double helix, see Bustamante et al. [7, 8] and Marko and Siggia [44], the Kradky and Porod model was recently adopted to simulate the behavior of the collagenous triple helix by Bischoff et al. [3, 4], Garikipati et al. [19, 20] and Kuhl et al. [37, 39].

After the collagen fibrils have formed in the extracellular space, they are greatly strengthened by the formation of covalent crosslinks between lysine residues of the constituent collagen molecules. If cross-linking is inhibited, the tensile strength of the fibrils is drastically reduced, the collagenous tissue becomes fragile and the structure tends to tear, see Alberts et al. [1]. To incorporate these characteristic cross-linking network effects, different isotropic chain network models have been proposed in the past, see, e.g., Flory [17], Treloar [53] and Arruda and Boyce [2, 5, 6]. In order to account for the

anisotropic nature of cardiovascular tissues on the mesoscopic extracellular matrix level, we generalize the cubic isotropic unit cell of the Arruda and Boyce model to obtain the orthotropic eight-chain model suggested recently by Bischoff et al. [3, 4].

Finally, it remains to incorporate the living nature of the tissue and its ability to adapt its collagenous microstructure to the mechanical loading environment. Naturally, fiber directions will evolve in vivo to optimize the load bearing capacity while keeping the required compliance. Traditionally, remodeling theories in arteries can be classified into stress driven and strain driven approaches. The former are typically based on the assumption that the cardiovascular tissue remodels its geometry to restore circumferential wall stress due to pressurization and wall shear stress due to blood flow to 'normal' levels, see, e.g., Taber and Humphrey [52], Gleason and Humphrey [22] or Hariton et al. [25]. Alternatively, motivated by successful predictions in hard tissue mechanics, the authors of the latter type of models suggest that strain rather than stress is the relevant driving force for the remodeling process, see Kuhl et al. [37], Himpel et al. [26] or Driessen et al. [13]. Either of the two theories is able to identify characteristic microstructural directions which are allowed to reorient with respect to the eigendirections of a mechanically relevant second-order tensor. In terms of algorithmic procedures, this vector reorientation typically leads to complex rotational updates which usually involve singularities due to the trigonometric nature of the underlying update equation, see, e.g., Menzel [45, 46]. Although very elegant from a mathematical point of view and maybe well-suited for microstructures with one predominant orientation, these reorientation models seem rather cumbersome in the context of arterial walls where multiple fiber families need to be accounted for.

When aiming to develop reliable constitutive theories for remodeling in cardiovascular tissues it is crucial to have detailed insight in the structural arrangement of the collagen fiber distribution. By using the birefringent properties of collagen, Finlay et al. [16] elaborated tangential sections of cerebral arterial walls to examine the integrated structural order of the individual layers. Alternative techniques providing information about the collagen fiber distribution in arterial walls were discussed recently by Elbischger et al. [14, 15]. Along these lines, continuously distributed collagen fiber orientations were incorporated in the more recent models by Driessen et al. [11, 12], Freed et al. [18] and Gasser et al. [21].

Experimental findings suggest that at biological equilibrium two predominant fiber orientations can be identified in each layer of the arterial wall. Typically, these two discrete families of collagen fibers are found to be located somewhere in between the directions of the two maximal principal stresses (or strains). Hence, as the stress (or strain) state varies with the radial position, the orientations of the two collagen fiber families also vary across the thickness of the arterial wall, as reported by, e.g., Taber and Humphrey [52] and Holzapfel et al. [30]. This variation across the wall thickness was successfully obtained from the discrete collagen fiber reorientation models by Driessen et al. [13] and Hariton et al. [25]. In [13] it was assumed that the collagen fibers align along preferred directions, situated in between the principal stretch directions, while in [25] the remodeling process was assumed to be stress driven. Within the present manuscript, we combine these basic assumptions with the fundamental concept of chain network models to obtain a three-dimensional remodeling theory which is general enough to predict remodeling in complex multiaxial loading situations. In contrast to existing theories, which strongly rely on complex rotational updates, this new approach can be algorithmically realized in terms of remarkably simple and straightforward updates of scalar-valued spatial dimensions.

The manuscript is organized as follows: the governing equations of the micromechanically motivated remodeling theory are derived in Sect. "Governing equations." Starting from the molecular level, we derive the constitutive equations for anisotropic soft biological tissues based on the concept of orthotropic chain network models. Section "Computational examples" then focuses on two particular model problems, a cylindrical tendon subject to uniaxial tension, and a tube-like artery subject to uniaxial stretch in combination with a distending pressure. Section "Discussion" closes with some final remarks.

Governing equations

In what follows, we summarize our set of constitutive equations for anisotropic cardiovascular tissues. To this end, we apply the following hypotheses:

- Hypothesis I: Large arteries seek to restore wall stress to within a range of homeostatic values.
- Hypothesis II: Collagen fibers as the main load bearing constituent of the extracellular matrix adapt their orientation and align with respect to the principal stress directions in order to minimize wall stress.
- Hypothesis III: Collagen fiber remodeling can be modeled and simulated phenomenologically to improve the understanding of fiber orientation and provide further insight in the structural arrangement of the individual arterial layers.

It should be mentioned, however, that although the present model takes into account microstructural information,

it is still based on a rather phenomenological approach in the sense that it does not explain the mechanisms how the individual cells actually sense changes in loading and communicate this information. Many different receptors on the surface of endothelial cells and vascular smooth muscle cells are able to detect subtle changes in the mechanical environment. They initiate various different mechanotransduction cascades according to the nature of the mechanical stimulus perceived. The cytoskeleton and other structural components play an important role in mechanotransduction as they are able to transmit and modulate tension between focal adhesion sites, integrins and the extracellular matrix. Moreover, changes in the mechanical environment may also initiate changes in the ionic composition of the cells, mediated by ion channels, stimulate various membrane receptors and induce complex biochemical responses, see, e.g., Huang et al. [31], Mofrad and Kamm [47] or Lehoux et al. [40] for excellent overviews. Since we do not aim at simulating these molecular mechanisms of mechanotransduction, all these phenomena are modeled phenomenologically through a set of continuum based remodeling equations which we describe in the sequel.

We begin on the microstructural level with the constitutive description of the individual collagen fibers. On the mesolevel, we then elaborate a representative volume element representing the extracellular matrix. On the macroscopic level, we finally characterize the overall tissue behavior through a micromechanically motivated constitutive model which is able to account for microstructural adaptation in response to changes in the mechanical loading.

On the collagen fiber level

On the microscopic level, we assume that the microstructure of a collagen triple helix is represented through the wormlike chain model. Wormlike chain models were introduced within the context of DNA mechanics by Marko and Siggia [44], and Bustamante et al. [7, 8], and recently applied to collagen fibers by Bischoff et al. [3, 4], Garikipati et al. [19, 20] and Kuhl et al. [37, 39]. In the statistical mechanics of long chain molecules such as collagen fibrils, the key kinematic variable that characterizes the conformation of the chain is the end-to-end length r. According to the wormlike chain model, the free energy ψ^{chn} of a single collagen fiber can be expressed in terms of the end-to-end length in the following form.

$$\psi^{\text{chn}} = \psi_0^{\text{chn}} + k\theta \frac{L}{4A}\left(2\frac{r^2}{L^2} + \frac{1}{1-r/L} - \frac{r}{L}\right) \tag{1}$$

Herein, ψ_0^{chn} is the value of the chain energy in the unperturbed state, $k = 1.381 \times 10^{-23}$ J/K is the Boltzmann constant and θ is the absolute temperature. In the case of living tissues, we suggest $\theta = 310$ K, i.e., $\theta = 37$ °C.

The two parameters governing the chain behavior are the contour length L and the persistence length A, as illustrated in Fig. 1.

The force required to pull the ends of the chain away from each other by a distance r thus follows straightforwardly by taking the derivative of the free energy ψ^{chn} with respect to the end-to-end length.

$$f^{\text{chn}} = \frac{\mathrm{d}\psi^{\text{chn}}}{\mathrm{d}r} = k\theta\frac{1}{4A}\left[4\frac{r}{L} + \frac{1}{(1-r/L)^2} - 1\right] \tag{2}$$

Note that due to the particular nature of the free energy ψ^{chn}, the end-to-end length r of a wormlike chain cannot extend beyond its contour length L as $0 < r < L$.

Remark 1 [Parameters on the collagen fiber level] The wormlike chain model is essentially a two-parameter model governed by the contour length L and the persistence length A. Figure 1 illustrates the physical meaning of the persistence length. It shows the force-displacement curves of a single collagen fiber indicating the increase in initial stiffness with increasing persistence length for, say, $A = 0.1$, $A = 0.4$, and $A = 0.8$. Note that throughout the entire manuscript, all lengths of the model have been rendered non-dimensional by dividing them by the link length of the chain, as proposed by Garikipati et al. [19].

Remark 2 [Specific data for the persistence length] F-actin (a filamentous protein responsible for the contraction and relaxation of muscle) has a persistence length A of approximately *16* μm. For nanotubes A is in

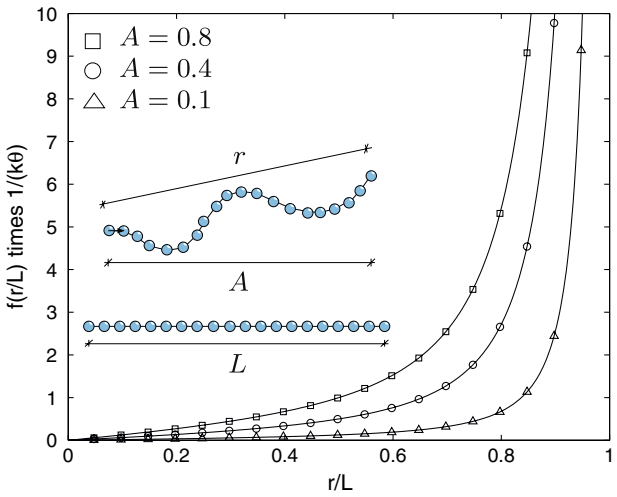

Fig. 1 Collagen fiber level ○ Single chain force vs. chain stretch for varying persistence lengths A

the millimeter range. Note, however, that A for DNA in vivo has a value of ~50 nm (Hagerman [24]), and A for synthetic polymers is typically only a few nanometers. Hence, the persistence lengths $A \ll L$ of a typical DNA molecule and a synthetic molecule are considerably smaller than their contour lengths L. Recent studies performed by means of optical tweezers seem to indicate that under physiological conditions collagen I molecules have a persistence length of ~14.5 nm which would be less than 5% of their contour length of ~309 nm, see Sun et al. [51]. Accordingly, collagen would be much more flexible than previously assumed, yet even more flexible than DNA. Although we suggest to stick to the wormlike chain approach in the sequel, this is not a general limitation of the overall constitutive model as such. Due to the modular structure of the overall framework, the free energy function for the individual fibers (1) can easily be modified, adapted and integrated straightforwardly in the macroscopic model.

On the extracellular matrix level

From a mechanical point of view, the extracellular matrix is modeled as a surrounding substrate in which the individual collagen fibers are embedded. A representative volume element of the extracellular matrix thus consists of a substrate of elastin, proteoglycans and cell, characterized through the isotropic free energy ψ^{iso}, and an anisotropic contribution due to the individual chains ψ^{chn}. Moreover, we introduce a repulsive chain contribution ψ^{rep} to characterize the tissue's behavior of the initial configuration such that the total free energy may be written in the following form.

$$\Psi = \Psi^{\text{iso}} + \Psi^{\text{chn}} + \Psi^{\text{rep}} \tag{3}$$

The individual terms of the free energy take on the explicit representations.

$$\begin{aligned}
\Psi^{\text{iso}} &= \frac{1}{2}\lambda \ln^2(J) + \frac{1}{2}\mu(I_1^C - n^{\text{dim}}) - \mu \ln(J) \\
\Psi^{\text{chn}} &= k\theta \frac{n^{\text{chn}} L}{4A}\left(2\frac{r^2}{L^2} + \frac{1}{1 - r/L} - \frac{r}{L}\right) \\
\Psi^{\text{rep}} &= k\theta \frac{n^{\text{chn}}}{4A}\left[\frac{1}{L} + \frac{1}{4r_0(1 - r_0/L)^2} - \frac{1}{4r_0}\right]\bar{\Psi}^{\text{rep}}
\end{aligned} \tag{4}$$

For the isotropic term Ψ^{iso}, we apply a standard neo-Hookean model expressed in terms of the first invariant $I_1^C = \boldsymbol{C} : \boldsymbol{I}$ of the right Cauchy-Green tensor $\boldsymbol{C} = \boldsymbol{F}^{\text{t}} \cdot \boldsymbol{F}$,where $\boldsymbol{F} = \nabla_X \varphi$ denotes the deformation gradient and $J = \det(\boldsymbol{F}) > 0$ is its determinant. Moreover, λ and μ are the standard Lamé constants.

The overall chain energy Ψ^{chn} follows by summing up the contributions ψ^{chn} of eight individual chains weightened by the overall chain number density n^{chn}, i.e., the number of chains per unit volume. According to the original eight-chain model by Arruda and Boyce, each of these chains connect the corners of a regular cuboid of dimensions 2 l_1, 2 l_2, and 2 l_3 with its center, compare Fig. 2, left. The end-to-end length r_0 in the undeformed configuration, thus, follows straightforwardly as $r_0 = \sqrt{l_I^2} = \sqrt{l_1^2 + l_2^2 + l_3^2}$. The unit cell is postulated to deform in the principal stretch space. Accordingly, the end-to-end length r in the deformed configuration can be expressed in terms of the deformation gradient $\boldsymbol{F}$ or rather in terms of the right Cauchy-Green tensor $\boldsymbol{C}$,

$$r = \sqrt{l_I^2 \bar{\boldsymbol{n}}_I \cdot \bar{\boldsymbol{n}}_I} = \sqrt{l_I^2 \boldsymbol{n}_I^0 \cdot \boldsymbol{C} \cdot \boldsymbol{n}_I^0} = \sqrt{l_I^2 \bar{I}_I^C} \tag{5}$$

with explicit summation over all three direction I = 1,2,3. Here, we have introduced the non-standard invariants $\bar{I}_I^C = \bar{\boldsymbol{n}}_I \cdot \bar{\boldsymbol{n}}_I = \boldsymbol{n}_I^0 \cdot \boldsymbol{C} \cdot \boldsymbol{n}_I^0$ with the understanding that $\bar{I}_I^C$ represents the stretch in the $\boldsymbol{n}_I^0$ direction squared. Thereby, $\boldsymbol{n}_I^0$ are the unit normal vectors of the unit cell axes in the undeformed reference configuration, see figure 3. After the deformation, they map onto the vectors $\bar{\boldsymbol{n}}_I = \boldsymbol{F} \cdot \boldsymbol{n}_I^0$ which are obviously no longer of unit length.

Finally, the repulsive contribution $\bar{\Psi}^{\text{rep}} = -\ln(\bar{I}_1^C \bar{I}_2^C \bar{I}_3^C)$ is constructed to compensate for the chain stresses in the reference configuration caused by non-vanishing initial

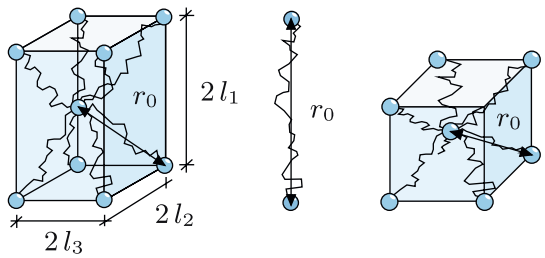

Fig. 2 Kinematics of the eight-chain model—orthotropic case (left), transversely isotropic case (middle), and isotropic case (right)

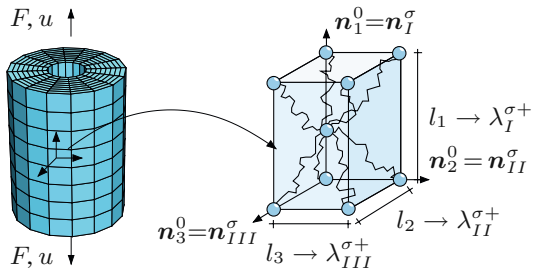

Fig. 3 Remodeling based on changes of cell dimensions ○ Instantaneous alignment of cell axes $\boldsymbol{n}_I^0$ with eigenvectors $\boldsymbol{n}_I^\sigma$ and gradual adaptation of cell dimensions $l_I$with respect to eigenvalues $\lambda_I^{\sigma+}$

end-to-end lengths r_0. Classically, the free energy Ψ introduced in (3) defines the Cauchy stress $\boldsymbol{\sigma}$ in the following form,

$$\boldsymbol{\sigma} = \frac{1}{J}\frac{\mathrm{d}\Psi}{\mathrm{d}\boldsymbol{F}} \cdot \boldsymbol{F}^{\mathrm{t}} = \boldsymbol{\sigma}^{\mathrm{iso}} + \boldsymbol{\sigma}^{\mathrm{chn}} + \boldsymbol{\sigma}^{\mathrm{rep}} \tag{6}$$

whereby the individual stress contributions can be expressed as follows.

$$\begin{aligned}
\boldsymbol{\sigma}^{\mathrm{iso}} &= \frac{1}{J}[\lambda \ln(J) - \mu]\boldsymbol{I} + \mu \boldsymbol{b} \\
\boldsymbol{\sigma}^{\mathrm{chn}} &= k\theta \frac{n^{\mathrm{chn}}}{4AJ}\left[\frac{1}{L} + \frac{1}{4r(1-r/L)^2} - \frac{1}{4r}\right]\bar{\boldsymbol{\sigma}}^{\mathrm{chn}} \\
\boldsymbol{\sigma}^{\mathrm{rep}} &= k\theta \frac{n^{\mathrm{chn}}}{4AJ}\left[\frac{1}{L} + \frac{1}{4r_0(1-r_0/L)^2} - \frac{1}{4r_0}\right]\bar{\boldsymbol{\sigma}}^{\mathrm{rep}}
\end{aligned} \tag{7}$$

Herein, the Finger deformation tensor $\boldsymbol{b} = \boldsymbol{F} \cdot \boldsymbol{F}^{\mathrm{t}}$ represents a characteristic spatial strain measure. The tensorial basis of the chain stress follows straightforwardly as $\bar{\boldsymbol{\sigma}}^{\mathrm{chn}} = l_I^2 \bar{\boldsymbol{n}}_I \otimes \bar{\boldsymbol{n}}_I$.Note that the repulsive energy Ψ^{rep} has been constructed such that the corresponding tensorial basis of the repulsive stress $\bar{\boldsymbol{\sigma}}^{\mathrm{rep}} = -l_I^2/\bar{I}_I^C \bar{\boldsymbol{n}}_I \otimes \bar{\boldsymbol{n}}_I$ ensures a stress free reference configuration as $\boldsymbol{\sigma}^{\mathrm{rep}} = -\boldsymbol{\sigma}^{\mathrm{chn}}|_{r=r_0}$ for which $\bar{I}_I^C = 1$ for all $I = 1,2,3$.

Remarks 3 [Special cases of transverse isotropy and isotropy] The orthotropic eight-chain model, as introduced by Bischoff et al. [3, 4], can be understood as a kinematic generalization of the original isotropic eight-chain model, as indicated in Fig. 2.

- Transverse isotropy $l_1 = r_0$ and $l_2 = l_3 = 0$ and thus $r = \sqrt{\bar{I}_1^C}\, r_0$
- Isotropy $l_1 = l_2 = l_3 = r_0/\sqrt{3}$ and thus $r = \sqrt{I_1^C/3}\, r_0$

The case of transverse isotropy follows by choosing $l_2 = l_3$, its yet more special case is the consideration of one single fiber direction $\boldsymbol{n}_1^0$ with $l_1 = r_0$ and $l_2 = l_3 = 0$. In this particular case, the end-to-end length $r = \sqrt{\bar{I}_1^C}\, r_0$ is obviously equivalent to the scaled stretch along the fiber direction $\boldsymbol{n}_1^0$. The special case of isotropy follows by assuming that all three cell dimensions are equal $l_1 = l_2 = l_3 = r_0/\sqrt{3}$ such that the end-to-end length $r = \sqrt{I_1^C/3}\, r_0$ can be expressed exclusively in terms of the trace of the right Cauchy-Green tensor $I_1^C = \boldsymbol{C} : \boldsymbol{I}$.

Remarks 4 [Parameters on the extracellular matrix level] On the extracellular matrix level, the mechanical behavior is characterized through eight parameters in total, i.e., Lamé constants λ and μ characterizing the surrounding substrate, the micromechanically motivated chain parameters L and A and the chain number density n^{chn}. For the moment, we shall assume the chain number density to be constant, however, its evolution in time due to changes in collagen content and thickness could be incorporated straightforwardly. The degree of anisotropy is governed by the unit cell dimensions l_1, l_2, and l_3 which implicitly define the end-to-end length $r_0 = \sqrt{l_I^2}$ in the initial configuration.

On the tissue level

In cardiovascular tissues, the collagen fibers are not arbitrarily distributed in space but follow rather a particular pattern. To account for remodeling in the form of microstructural rearrangement, we allow the fiber direction to rotate in response to the current mechanical stress environment. We assume the Cauchy stress tensor

$$\boldsymbol{\sigma} = \lambda_I^\sigma \boldsymbol{n}_I^\sigma \otimes \boldsymbol{n}_I^\sigma \tag{8}$$

to be the driving force of the remodeling process. Here, we have introduced its eigenvalue decomposition with λ_I^σ and $\boldsymbol{n}_I$ being the corresponding eigenvalues and eigenvectors, respectively. For notational simplicity, we have implicitly assumed the summation over all $I = 1,2,3$ components. Our remodeling theory is based on two fundamental hypotheses:

- Hypothesis I: The characteristic directions $\boldsymbol{n}_I^0$ of the microstructure align instantaneously with respect to the eigenvectors $\boldsymbol{n}_I^\sigma$.
- Hypothesis II: The unit cell dimensions l_I adapt gradually with respect to the positive eigenvalues $\lambda_I^{\sigma+}$.

The first postulate is motivated by the general idea beyond all network models that the unit cell is taken to deform in the principal stretch space, see, e.g., Boyce and Arruda [6]. The second postulate closely follows the recent approach of Hariton et al. [25] suggesting that the collagen fibers in cardiovascular tissues are located between the directions of the two maximum principal stresses. Accordingly, the essence of our remodeling theory can be summarized as follows,

$$\boldsymbol{n}_I^0 \equiv \boldsymbol{n}_I^\sigma \quad \text{and} \quad l_I \to r_0 \frac{\lambda_I^{\sigma^+}}{||\lambda_I^{\sigma^+}||} \tag{9}$$

compare with Fig. 3. For the sake of notational simplicity, we have introduced the notion $\lambda_I^{\sigma^+}$ with the understanding that $\lambda_I^{\sigma^+} = \lambda_I^\sigma$ for positive eigenvalues $\lambda_I^\sigma > 0$ and $\lambda_I^{\sigma^+} = 0$ for non-positive eigenvalues $\lambda_I^\sigma \leq 0$. From a physiological point of view, we thus exclusively allow for tension driven reorientation processes. It remains to formulate a reasonable evolution equation for the microstructural cell dimensions l_I which we assume to obey the following law

$$\mathrm{d}_t l_I = \kappa\left(\frac{\lambda_I^{\sigma+}}{||\lambda_I^{\sigma+}||} - \frac{l_I^0}{r_0}\right)\exp(-\kappa t) r_0 \tag{10}$$

where κ denotes a relaxation parameter and l_I^0, $I = 1,2,3$, are the dimensions of the cuboid in the undeformed configuration. Alternatively, the above equation could be integrated in time to render an explicit update equation for all cell dimensions l_I.

$$l_I = \left(\frac{\lambda_I^{\sigma+}}{||\lambda_I^{\sigma+}||} - \frac{l_I^0}{r_0}\right)[1 - \exp(-\kappa t)] r_0 + l_I^0 \tag{11}$$

Recall that the reorientation process itself leaves the initial chain length $r_0 = \sqrt{l_I^2}$ unaltered.

Remarks 5 [Remodeling based on fiber rotation] Previous remodeling approaches in the literature focused on the reorientation of a single microstructural direction, see, e.g., Menzel [46], Kuhl et al. [37] and Himpel et al. [26]. Applications thus focused primarily on transversely isotropic biological tissues with one distinguished fiber orientation such as muscles, tendons or ligaments for which $l_2 = l_3 \ll l_1$. Similar to the previous approach, reorientation was assumed to be driven by either strain or stress, based on an eigenvalue decomposition, as given in (8). In contrast to the new model suggested in this contribution, the following assumptions were postulated for the remodeling process:

- The characteristic direction $\boldsymbol{n}_1^0$ of the microstructure aligns gradually with respect to the eigenvector $\boldsymbol{n}_{\max}^{\sigma}$ related to the maximum positive eigenvalue $\lambda_{\max}^{\sigma+}$.
- The unit cell dimensions l_I remain unaffected by the process of remodeling.

Consequently, the reorientation-based analogue of Eq. (9) could be expressed as follows, compare Fig. 4.

$$\boldsymbol{n}_1^0 \to \boldsymbol{n}_{\max}^{\sigma} \quad \text{and} \quad l_I = \text{const.}$$

Rather than updating the scalar-valued unit cell lengths l_I, this reorientation approach requires an update of the vector-valued fiber direction $\boldsymbol{n}_I^0$

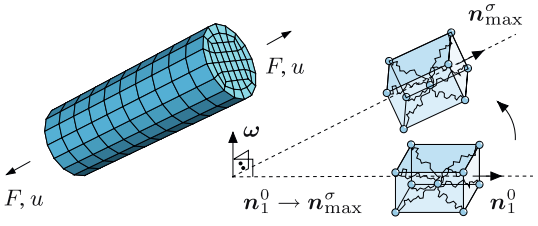

Fig. 4 Remodeling based on changes of cell orientation ○ Gradual alignment of the cell axes $\boldsymbol{n}_1^0$ with eigenvector $\boldsymbol{n}_{\max}^{\sigma}$ of related maximum principal eigenvalue $\lambda_{\max}^{\sigma+}$ and constant cell dimensions l_I = const

$$\mathrm{d}_t \boldsymbol{n}_1^0 = \boldsymbol{\omega} \times \boldsymbol{n}_1^0$$

which is obviously more cumbersome due to numerical singularities introduced through trigonometric functions. In contrast to the rather simple explicit equation for the adaptation of the unit cell dimensions (11), the fiber direction can be expressed through the exponential update

$$\boldsymbol{n}_1^{0k+1} = \exp(-\Delta t \overset{3}{\boldsymbol{e}} \cdot \boldsymbol{\omega}) \cdot \boldsymbol{n}_1^{0k} \qquad \boldsymbol{\omega} = \frac{1}{\kappa}\boldsymbol{n}_1^{0k+1} \times \boldsymbol{n}_{\max}^{\sigma}$$

where $\boldsymbol{\omega}$ and $\overset{3}{\boldsymbol{e}}$ denote the time discrete rotation vector and the third-order permutation tensor, respectively. Recall that in addition to potential numerical difficulties, this previous reorientation approach is restricted to transversely isotropic biological tissues and its extension to reorienting multiple directions seems to be a rather complex task.

Remarks 6 [Dissipation] It is a well-accepted fact that a purely mechanical theory is thermodynamically inadmissible for remodeling processes that stiffen the material, see, e.g., the discussions in Menzel [46], Kuhl et al. [37], and Himpel et al. [26] or Garikipati et al. [20]. The fact that the dissipation would be positive for stiffening materials in a purely mechanical theory indicates that other thermodynamic phenomena, e.g., of chemo-mechanical nature, should indeed be taken into account. Alternatively, mixture theories could be considered in which energy and entropy are exchanged amongst the individual constituents of the tissue, see, e.g., Gleason and Humphrey [22, 23]. Accordingly, to date, there is no general agreement of how evolution laws for reorientation of microstructural directions should be formulated. In the context of linear elasticity, it has been shown that the free energy attains an extremum if strain and stress share the same principal directions, see, e.g., Cowin [10] or Vianello [54]. In non-linear elasticity, however, it is not even clear to date whether stress or strain is the relevant driving force for the remodeling process. The previous $\boldsymbol{n}_1^0 \to \boldsymbol{n}_{\max}^{\sigma}$ non-linear reorientation model addressed in *Remark 5* is based on the general paradigm that nature always tries to find the extremum, see Menzel [46], Kuhl et al. [37] and Himpel et al. [26]. However, the recent reorientation model for arteries by Hariton et al. [25] just postulated a general stress driven remodeling process and so does the model presented herein. For detailed discussions about the impact of the dissipation inequality in remodeling, the reader is referred to the excellent discussion by Garikipati et al. [20].

Remarks 7 [Parameters on the tissue level] An additional convincing benefit of the incorporation of remodeling is

that the number of parameters could even be reduced, as compared to the fixed cell dimension model introduced in Sect. "Governing equations." For the overall model of adapting living tissue, seven material parameters are required altogether, i.e., the two Lamé constants λ and μ for the extracellular matrix, the chain number density n^{chn}, the micromechanically motivated contour length L and the persistence length A. However, now, instead of prescribing fixed cell dimensions l_1, l_2, and l_3, we just have to define the initial chain length r_0, while the individual dimensions of the cell evolve naturally in response to the given mechanical loading environment.

Nevertheless, one additional parameter κ is introduced to account for the speed of adaptation. From a biological point of view, the relaxation parameter κ reflects the turnover rate or rather the speed of adaptation. Note that we have implicitly assumed that the time scale for fiber reorientation is orders of magnitude larger than the typical time scale of a diastolic-systolic pressure circle. The role of κ is illustrated in Fig. 5 for a simulation with $\lambda = 27.293$, $\mu = 3.103$, $n^{\text{chn}} = 7.0 \times 10^{21}$ chains per unit volume, $L = 2.125$, $A = 1.82$, and $r_0 = 1.0$. In the initial state, we assume an isotropic fiber distribution with $l_1 = l_2 = l_3 = r_0/\sqrt{3}$. The curves illustrate the angle of alignment for a cubic specimen of unit length subject to uniaxial tension with an incremental loading of $\Delta F = 1.0$. The load is applied in 10 steps in the dimensionless time interval $0 < t \leq 10$. Then, at $F = 10.0$, the load is held constant while the cell dimensions are allowed to remodel progressively at $10 < t \leq 100$. Figure 5 demonstrates that the collagen fibers align gradually with respect to the loading axis. As time evolves, $l_1 \rightarrow r_0$ while $l_2 = l_3 \rightarrow 0$ whereby $\boldsymbol{n}_1^0$ is instantaneously aligned with the loading axis. As expected, the speed of the adaptation process increases for larger values of the relaxation parameter κ.

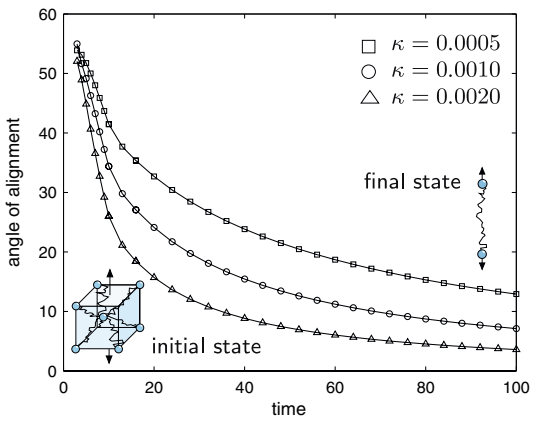

Fig. 5 Tissue level ○ Angle between collagen fibers and direction of uniaxial tension versus time for varying relaxation parameters κ

Computational examples

Finally, the features of the proposed remodeling strategy is elaborated by means of two benchmark problems, i.e., a cylindrical tendon subject to uniaxial tension, and a tube-like artery subject to uniaxial stretch in combination with internal pressure.

Since we aim at elaborating inhomogeneous structures with an initially random fiber orientation, the remodeling strategy is embedded in a standard finite element algorithm with the remodeling equation being evaluated at the integration point level. A Newton–Raphson solution strategy based on a consistent linearization of the governing equations is applied throughout to solve the non-linear biomechanical problem efficiently in an incrementally iterative way.

In the following examples, we choose the Lamé parameters to $\lambda = 27.293$ and $\mu = 3.103$ according to Menzel [45]. The Boltzmann constant is $k = 1.381 \times 10^{-23}$, and the absolute temperature is $\theta = 310$, measured in Kelvin. Recall that all chain lengths are normalized by a length scale originating from the statistical model. Following Garikipati et al. [19], we scale all lengths by the link length in a chain. Accordingly, the contour length is chosen to be $L = 1.594$, the corresponding persistence length that accounts for a reasonable initial stiffness is $A = 1.365$, and the initial end-to-end length is $r_0 = \sqrt{l_I^2} = 1.0$. The degree of anisotropy is reflected through the chain number density n^{chn}, i.e., the number of chains per unit volume, which we choose in the order of 10^{21}, as suggested by Bischoff et al. [3] or Garikipati et al. [19], thus $n^{\text{chn}} = 2 \times 10^{21}$. The relaxation parameter is chosen to be $\kappa = 0.025$ per unit time. In all examples, we start with an initially random fiber orientation which is realized by assigning different values to the unit cell dimensions l_I in each element of the mesh. Due to the geometric and material non-linearities of the problem, the load is applied incrementally until the final load level is reached. Then, the load is held constant while remodeling occurs until convergence towards a biological equilibrium state.

Cylindrical tendon under uniaxial tension

To elaborate the proposed remodeling algorithm in the simple case of uniaxial loading, we analyze a cylindrical tendon under uniaxial tension which has been studied earlier in the context of tissue engineering of tendon constructs by Kuhl et al. [37]. When strained along its load-bearing axis, tendon shows a microscopical straightening of the low amplitude wavy collagen fibers accompanied by an exponentially increasing resistance to elongation. The model tendon we aim at analyzing qualitatively to elaborate whether the suggested model is able to

capture these general trends is 10 units long and has an initial cross-section of 10 units^2. It is discretized with 10 elements in height and 48 elements per cross-section, thus with 480 tri-linear finite elements in total. The load is increased incrementally with $\Delta F = 25$ from $0 < t \leq 12$ until a final load level of $F = 300$ is reached. From $12 < t \leq 150$, we apply another 138 remodeling steps until biological equilibrium occurs.

Figure 6 illustrates the remodeling history of the cylindrical tendon. At first, when the load is applied, the tendon is stretched in the axial direction up to about 175% of its original length, compare with Fig. 6, left. However, as time evolves, the collagen fibers tend to align gradually with the loading axis. Accordingly, the structure stiffens significantly and the overall stretch decreases to about 140%. At the final and yet stiffest state, all fibers are aligned with the direction of the mechanical load.

During the remodeling process, the unit cell lengths have obviously evolved from initially random values $0 \leq l_I \leq r_0$ with $\sqrt{l_I^2} = r_0$ to $l_1 = r_0$ and $l_2 = l_3 = 0$ representing the special case of transverse isotropy. Selected snapshots of the remodeling history are depicted in Fig. 6, right. For each element, the end-to-end vectors of each chain have been projected on the tendon's surface. The individual colors represent the collagen fiber angle measured against the loading axis. Red colors indicate a full alignment with an angle zero, while blue colors indicate that the collagen fibers are oriented orthogonal to the loading axis. In particular, in the second snapshot of the series at $t = 12$ corresponding to the final loading state, the spatial inhomogeneity is nicely visible. The red elements with aligned collagen fibers display very stiff response and deform only marginally while the soft blue elements undergo significant stretches. As expected, this initial inhomogeneity tends to vanish gradually in the course of remodeling.

Tube-like artery subject to uniaxial stretch and internal pressure

We turn now to the more challenging example of a multiaxial loading state induced by a uniaxial stretching in combination with an internal pressure representing the blood flow. It has long been recognized that the layered structure of cardiovascular tissues displays a geometric complexity way beyond the highly organized parallel bundles of collagen fibers that constitute the mechanical backbone of tendons. Motivated by earlier theoretical studies of Driessen et al. [13] and Hariton et al. [25], and supported by the experimental findings of Finlay et al. [16], we analyze the remodeling history in a tube-like artery. At this point, we restrict ourselves to a rather qualitative analysis aiming at including physiologically realistic data at later stages of this project. The initial dimensions are given through a length of 8 units and an inner and outer radius of 1 and 3 units, respectively. Along the height we apply 12 elements, we use 8 elements across the thickness and 16 elements in circumferential direction. Here, we apply standard tri-linear finite elements. Note, however, that shell elements would be more appropriate when it comes to quantitative studies. The load is applied incrementally in 25 load steps from $0 < t \leq 25$ with $\Delta p = 0.192\, p_0$ and $\Delta l = 0.032$ until a final state of $p = 4.8\, p_0$ and $\Delta l = 0.8$, i.e., an axial stretch of 10%, is reached. Again, the load is then held constant for another 125 time steps for the time period $25 < t \leq 150$ to allow for remodeling towards a final state of biological equilibrium. Figure 7 shows five selected snapshots of the remodeling process. In between the first and the second snapshot, the internal pressure and the prescribed axial stretch are increased incrementally. Accordingly, the tube blows up and stretches along its axial direction occur. Due to the nearly incompressible behavior of soft biological tissues, the tube thickness decreases drastically in response to loading. As time evolves, the collagen fibers tend to reorient so that they are finally located between the two directions of maximum principal stress. For this particular case of loading, these are obviously the longitudinal and the circumferential directions.

Starting from an initial random orientation at random unit cell lengths $0 \leq l_I \leq r_0$ with $\sqrt{l_I^2} = r_0$ in the first snapshot of the series, the unit cell lengths evolve progressively driven by the positive eigenvalues of the Cauchy stress $\lambda_I^{\sigma+}$. As a natural consequence, the chain directions remodel gradually and the tube stiffens with respect to the

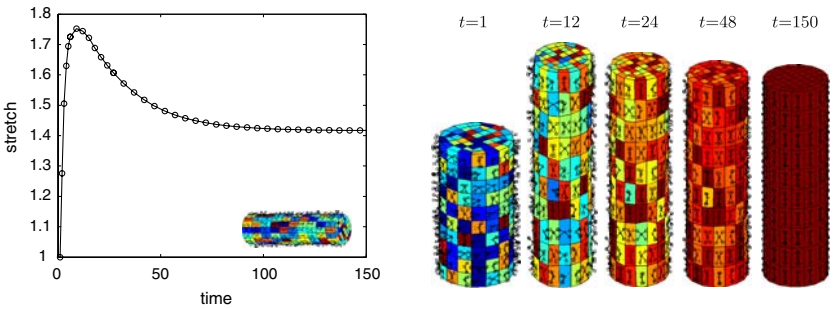

Fig. 6 Cylindrical tendon under uniaxial tension ○ Stretch versus time (left) and selected snapshots of the remodeling process at different times with colors representing the individual collagen fiber angles (right)

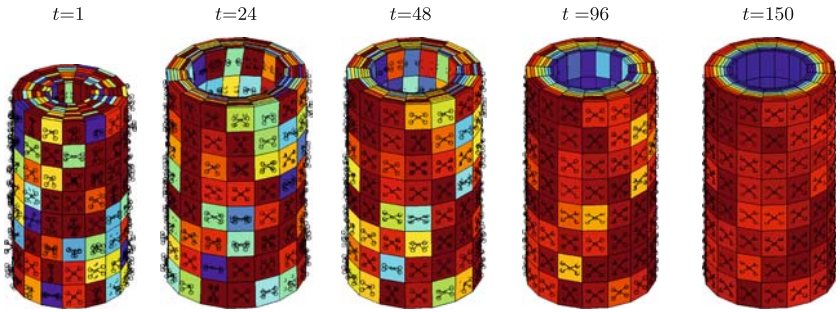

Fig. 7 Tube-like artery subject to axial stretch and internal pressure ○ Selected snapshots of the remodeling process at different times with colors representing the individual collagen fiber angles

applied loading. Accordingly, the outer radius, which had increased during the first stages of loading, decreases remarkably in response to remodeling, compare time $t = 24$ with $t = 150$. While the chains had originally been oriented randomly in space at $t = 1$, their component in radial direction vanishes gradually as l_3 goes to zero in response to the compressive stresses $\lambda_3^{\sigma} \leq 0$ in the radial direction at $t = 150$. Thus, the suggested remodeling algorithm proves able to produce not only transversely isotropic but also orthotropic microstructures in a natural way.

Recall that the final collagen fiber angles developed naturally in response to the positive eigenvalues $\lambda_I^{\sigma+}$ of the Cauchy stress $\boldsymbol{\sigma}$ which had been postulated to be the driving force of the remodeling process. Due to the inhomogeneous stress state across the radial direction, different fiber angles arise in the individual layers.

Figure 8 depicts the final collagen fiber orientations at three different radial locations representing the intima, the media and the adventitia. The results suggest that the transmural pitch of the fiber orientation increases from the inner to the outer wall. The analytically predicted double-helix architecture of the collagen fibers agrees very well with experimental observations by Finlay et al. [16] and Holzapfel et al. [27, 30]. In addition, our results nicely agree with the more recent numerical studies by Driessen et al. [13] and Hariton et al. [25].

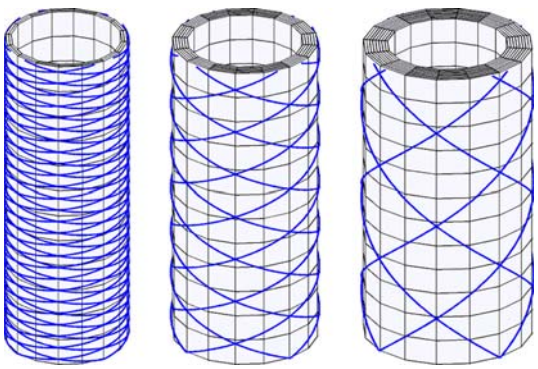

Fig. 8 Tube-like artery subject to axial stretch and internal pressure ○ Final stage of the remodeling process with collagen fiber orientations projected on the individual layers

The predicted inhomogeneity in the radial direction with an almost circumferential fiber orientation at the luminal side of the artery and an increase of the inclination towards the outer side is closely related to the phenomenon of prestress, typically encountered in arterial specimens. For the considered model problem, the degree of inhomogeneity, obviously, strongly depends on the stretch-to-pressure ratio. Motivated by a recent study by Gleason and Humphrey [23] who analyzed the elastin, collagen and smooth muscle cell turnover and remodeling in response to different loading scenarios, we systematically elaborate combinations of transmural pressure and axial stress. To illustrate the influence of the mechanical loading situation on the remodeling process, we display Fig. 9 to show the final biological equilibrium stages for different stretches at different pressure levels. For the sake of visibility, we have virtually peeled off the individual layers after the calculation of the entire tube had been performed. Experimentally, the definition of these specific layers could be made apparent by the use of stains differentiating smooth muscles cells from collagen fibers. For pure stretching, as depicted in Fig. 9 (left), the fibers of all layers are aligned with the loading axis, i.e., $l_1 = r_0$ and $l_2 = l_3 = 0$ with $\boldsymbol{n}_1^0$ pointing in the axial direction. For pure pressure, as depicted in Fig. 9 (right), all fibers are oriented in the circumferential direction, i.e., again, $l_1 = r_0$ and $l_2 = l_3 = 0$, however, now with $\boldsymbol{n}_1^0$ pointing in the circumferential direction. These computational results agree well with the experimental findings of human brain arteries by Finlay et al. [16] who reported a significant realignment of collagen with increasing distending pressure for all arterial layers and a recruitment towards the circumferential direction. Intermediate stages of combined stretch and pressure loading, as shown in the three images between the left and the right image of Fig. 9, reveal the usually observed helical fiber arrangement. Based on these results, it is obvious to suggest that the collagenous architecture strongly depends on the mechanical environment.

In the biomechanics community there is an ongoing debate over which quantity drives the remodeling process. To this end, we analyze the influence of different driving forces of tensorial nature. For purpose of comparison with

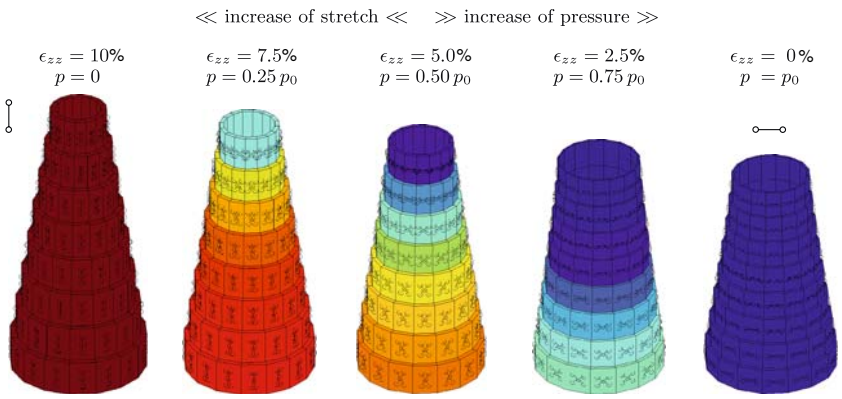

Fig. 9 Tube-like artery subject to axial stretch and internal pressure ○ Variations of collagen fiber orientations in response to different stretch-to-pressure ratios with colors representing the individual collagen fiber angles

the (spatial) Cauchy stress $\boldsymbol{\sigma}$ used in the previous examples, we now elaborate the use of the (material) second Piola–Kirchhoff stress $\boldsymbol{S} = J\boldsymbol{F}^{-1} \cdot \boldsymbol{\sigma} \cdot \boldsymbol{F}^{-\mathrm{t}}$, as the representative material stress measure. Figure 10 compares now the outcome of a remodeling process driven by spatial and material stresses. The diagram illustrates the fiber orientation angle over the radius. Variations in fiber orientation seem to be slightly more pronounced when using the second Piola–Kirchhoff stress as the driving force. Nevertheless, for this particular problem, it appears that differences are rather marginal. We suggest that the Cauchy stress, which is the true stress experienced by the deformed structure, is the more reasonable choice.

Finally, we elaborate the difference of a stress and strain-based remodeling criterion, as used by, e.g., Driessen et al. [13], Menzel [46] and Humphrey [32], Hariton et al. [25], respectively. To this end, we compare the outcome of two different remodeling processes based on either the Cauchy stress $\boldsymbol{\sigma}$ as the characteristic spatial stress measure, see Fig. 11 (left), or on the Finger deformation tensor $\boldsymbol{b}$ as the characteristic spatial strain measure, see Fig. 11 (right). Both the curves as well as the plots of the structure demonstrate that strain-based remodeling is much less sensitive to the radial variation. The difference between an almost circumferential arrangement at the luminal side and a rather helical structure towards the outermost layer is less

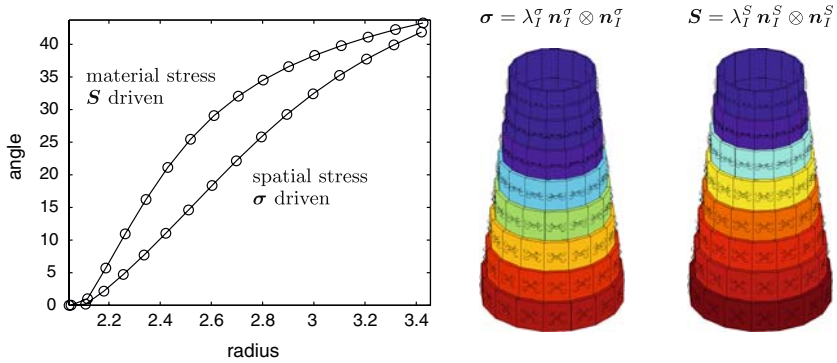

Fig. 10 Tube-like artery subject to axial stretch and internal pressure ○ Collagen fiber orientation versus radial position (left) and outcome of spatial versus material stress-based remodeling (right)

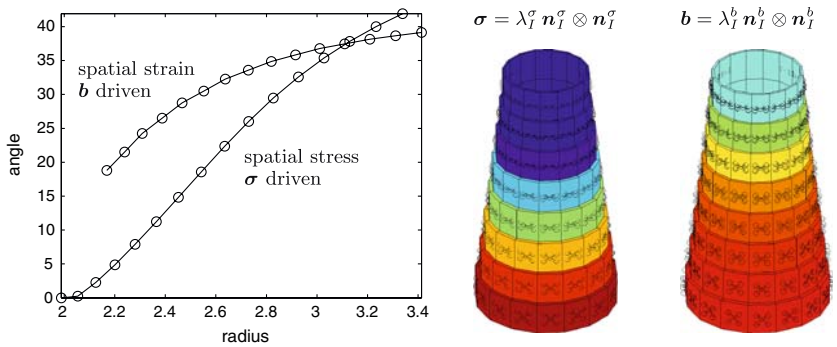

Fig. 11 Tube-like artery subject to axial stretch and internal pressure ○ Collagen fiber orientation versus radial position (left) and outcome of spatial stress versus spatial strain-based remodeling (right)

pronounced for the strain driven case. This finding is, of course, rooted in the non-linear nature of the force-displacement behavior of the individual chains, recall Fig. 1. While the strain varies slowly close to the locking stretch, corresponding stresses may vary significantly. Accordingly, the stress-based remodeling criterion predicts a wider variation in collagen fiber angles than the strain driven remodeling algorithm. Although for hard tissues, such as bone, several studies including the one by Cowin [9] suggest that strain is the critical mechanical factor in growth and adaptation, we postulate that stress is a more reasonable choice as the driving force in the context of soft tissues such as arteries, tendons or ligaments. This observation is along with Taber and Humphrey [52] who suggest that stress and not strain correlates well with growth in arteries.

Discussion

A continuum theory of remodeling for soft biological tissues has been proposed with a particular focus on cardiovascular tissue. In this context, remodeling is attributed to the collagen fiber reorientation as a natural consequence of changes in the mechanical loading environment. Hence, in our approach the optimal configuration of collagen fibers depends solely on the external loading acting upon the living tissue. Based on a homogenization strategy from the molecular microscale via the mesoscale of the extracellular matrix to the macroscale of the overall tissue, we derived a statistical mechanics-based chain network model governed by a limited set of physically motivated material parameters. In addition to the two (classical) Lamé constants, five additional parameters sufficed to characterize the highly non-linear, exponentially stiffening of the collagen morphology: the contour length, the persistence length and the initial end-to-end length of the collagen chains, the chain number density accounting for the degree of anisotropy and the turnover rate. The concept of chain network models was applied to transmit information from the molecular level to the extracellular matrix level. In contrast to existing remodeling theories which are based on complex rotational updates of characteristic microstructural directions, our theory essentially captures remodeling in the form of changes of the dimensions of this representative element. By means of simple model problems, we were able to show that the theory indeed succeeded in characterizing mechanically introduced remodeling of collagen fibers.

Finally, we elaborated two biomechanically relevant boundary-value problems, a cylindrical tendon subject to uniaxial tension and a tube-like artery loaded by an axial stretch in combination with different internal pressures. For these more complex inhomogeneous (living) structures, the remodeling algorithm was embedded in a non-linear finite element program, the equations were linearized consistently and solved with an incremental iterative Newton–Raphson solution strategy. Starting with initially random fiber orientation, the algorithm generated collagenous architectures which qualitatively resembled experimental observations. In all computational examples, the suggested algorithm convinced through its remarkable stability and robustness. What remains, however, is the realization of quantitative validations of the suggested theory and its algorithmic realization. In addition to the collagen fiber orientation, which could eventually be determined through techniques such as microscopy, histology, magnetic resonance diffusion tensor imaging, the chain number density and the turnover rate remain to be classified. The latter is assumed to be of particular relevance in the context of improving cardiovascular surgery and predicting patient-specific remodeling in response to medical treatment.

Finally we would like to point out once again, that although the reorientation approach outlined in the present manuscript is motivated by micromechanical considerations, it is still rather phenomenological to most extend. In contrast to purely invariant based formulations, it introduces material parameters such as the contour length or the persistence length which have a clear physical interpretation. The computational mechanics community would thus certainly classify the model as bottom-up or rather micromechanically based and non-phenomenological. In the cell biology community, however, the same model would most probably be considered rather phenomenological or top-down since it does not explicitly address cell level phenomena like mechanotransduction or the biochemical origin of the remodeling process as such. Nevertheless, to date it seems unmanageable to simulate large tissue structures or organs and yet at the same time to account for every single biochemical phenomenon individually. To the most extend, these complex mechanisms are not even fully understood at this point.

Successful constitutive models require an understanding of the functional interactions between the key components of cells up to the organs, and how these interactions change from a physiological to a pathological state. Such information resides neither in the individual genome nor in the protein. This information is contained in the interactions of proteins with cellular, organ and system structures. The identification of these interactive relationships is clearly within the focus of intense current research. Continuum models like the one presented herein will certainly benefit from gradually incorporating more and more information from the protein, subcellular and cellular level in the future to define precisely how mechanical forces translate into chemical signals that initiate the process of remodeling.

References

1. Alberts B, Johnson A, Lewis J, Raff M, Roberts K, Walter P (2002) Molecular biology of the cell, 4th edn. Garland Science Taylor Francis Group, New York
2. Arruda EM, Boyce MC (1993) J Mech Phys Solids 41:389
3. Bischoff JE, Arruda EM, Grosh K (2002) J Appl Mech 69:570
4. Bischoff JE, Arruda EM, Grosh K (2002) J Appl Mech 69:198
5. Boyce MC (1996) Rubber Chem Technol 69:781
6. Boyce MC, Arruda EM (2000) Rubber Chem Technol 73:504
7. Bustamante C, Bryant Z, Smith SB (2003) Nature 421:423
8. Bustamante C, Smith S, Marko JF, Siggia ED (1994) Science 265:1599
9. Cowin SC (1984) Calc Tissue Int 36:S99
10. Cowin SC (1995) J Elast 34:45
11. Driessen NJB, Bouten CVC, Baaijens FPT (2005) J Biomech Eng 127:494
12. Driessen NJB, Peters GWM, Huyghe JM, Bouten CVC, Baaijens FPT (2003) J Biomech 36:1151
13. Driessen NJB, Wilson W, Bouten CVC, Baaijens FPT (2004) J Theor Biol 36:53
14. Elbischger PJ, Bischof H, Holzapfel GA, Regitnig P (2005) In: Suri JS, Yuan C, Wilson DL, Laxminarayan S (eds) Plaque imaging: pixel to molecular level, vol 113. Studies in Health Technology and Informatics, IOS Press, p 97
15. Elbischger PJ, Bischof H, Regitnig P, Holzapfel GA (2004) Pattern Anal Appl 7:269
16. Finlay HM, Mc Cullough L, Canham PB (1995) J Vasc Res 32:301
17. Flory PJ (1969) Statistical mechanics of chain molecules. John Wiley Sons, Chichester–New York
18. Freed AD, Einstein DR, Vesely I (2005) Biomech Model Mechanobiol 4:100
19. Garikipati K, Arruda EM, Grosh K, Narayanan H, Calve S (2004) J Mech Phys Solids 52:1595
20. Garikipati K, Olberding JE, Narayanan H, Arruda EM, Grosh K, Calve S (2006) J Mech Phys Solids 54:1493
21. Gasser TC, Ogden RW, Holzapfel GA (2006) J R Soc Interface 3:15
22. Gleason RL, Humphrey JD (2004) J Vasc Res 41:352
23. Gleason RL, Humphrey JD (2005) Math Med Biol 22:347
24. Hagerman PJ (1988) Annu Rev Biophys Biophys Chem 17:265
25. Hariton I, de Botton G, Gasser TC, Holzapfel GA (2006) Biomechanics and modeling in mechanobiology, pp available online, DOI 10.1007/s10237-006-0049-7
26. Himpel G, Menzel A, Kuhl E, Steinmann P (2007) Int J Num Meth Eng, in press
27. Holzapfel GA, Gasser TC, Stadler M (2002) European J Mech A Solids 21:441
28. Holzapfel GA, Ogden RW (2003) Biomechanics of soft tissue in cardiovascular systems CISM courses and lectures no 441. Springer Verlag, Wien–New York
29. Holzapfel GA, Ogden RW (2006) mechanics of biological tissue. Springer, Berlin–Heidelberg–New York
30. Holzapfel GA, Stadler M, Schulze-Bauer CAJ (2002) Ann Biomed Eng 30:753
31. Huang H, Kamm R, Lee RT (2003) Am J Physiol Cell Physiol 287:C1
32. Humphrey JD (2001) J Biomech Eng 123:638
33. Humphrey JD (2002) Cardiovasular solid mechanics. Springer Verlag, Berlin–Heidelberg–New York
34. Ingber DE (2003) Ann Intern Med 35:564
35. Klein-Nulend J, Bacabac RG, Mullender MG (2005) Pathol Biol (Paris) 53:576
36. Kratky O, Porod G (1949) Recl Trav Chim 68:1106
37. Kuhl E, Garikipati K, Arruda EM, Grosh K (2005) J Mech Phys Solids 53:1552
38. Kuhl E, Maas R, Himpel G, Menzel A (2006) Biomechanics and modeling in mechanobiology, pp available online, DOI 10.1007/s10237-006-0062-x
39. Kuhl E, Menzel A, Garikipati K (2006) Phil Mag 86:3241
40. Lehoux S, Castier Y, Tedgui A (2006) J Intern Med 259:381
41. Leung DYM, Glagov S, Mathews MB (1976) Science 191:475
42. Leung DYM, Glagov S, Mathews MB (1977) Circ Res 41:316
43. Lubarda VA, Hoger A (2002) Int J Solids Struct 39:4627
44. Marko JF, Siggia ED (1995) Macromolecules 28:8759
45. Menzel A (2006) In: Holzapfel GA, Ogden RW (eds) IUTAM Symposium mechanics of biological tissue. Springer Verlag, p 91
46. Menzel A (2005) Biomech Model Mechanobiol 3:147
47. Mofrad MRK, Kamm R (eds) (2006) Cytoskeletal mechanics models and measurements. Cambridge University Press
48. Nerem RM, Seliktar D (2001) Annu Rev Biomed Eng 3:225
49. Rodriguez EK, Hoger A, Mc Culloch AD (1994) J Biomech 27:455
50. Stopak D, Harris AK (1982) Dev Biol 90:383
51. Sun YL, Luo ZP, Fertala A, An KN (2002) Biochem Biophys Res Commun 295:382
52. Taber LA, Humphrey JD (2001) J Biomech Eng 123:528
53. Treloar LRG (1975) The physics of rubber elasticity. Clarendon Press, Oxford
54. Vianello M (1996) J Elast 42:283
55. Wang JH, Thampatty BP (2006) Biomech Model Mechanobio 5:1